CFD Analysis of a Partial Admission Turbine Using a Frozen Rotor Method

Jun Gu Noh, Eun Seok Lee, Jinhan Kim, Dae Sung Lee
Turbopump Dept. Korea Aerospace Research Institute
45 Eoeun-Dong Yuseong-Gu Daejeon 305-333 Korea
ESL@kari.re.kr

Keywords: Turbopump, Partial Admission Turbine, Rotor/Stator Interaction, Frozen Rotor Method

Abstract

A numerical flow analysis has been performed on the partial admission turbine of KARI turbopump to support the aerodynamic and structural dynamic assessments. The flow-field in a partial admission turbine is essentially three dimensional and unsteady because of a tip clearance and a finite number of nozzles. Therefore the mixing plane method is generally not appropriate. To avoid heavy computational load due to an unsteady three dimensional calculation, a frozen rotor method was implemented in steady calculation. It adopted a rotating frame in the grid block of a rotor blade by adding some source terms in governing equations. Its results were compared with a mixing plane method. The frozen rotor method can detect the variation of flow-field dependent upon the blade's circumferential position relative to the nozzle. It gives a idea of wake loss mechanism starting from the lip of a nozzle. This wake loss was assumed to be one of the most difficult issues in turbine designers. Thus, the frozen rotor approach has proven to be an efficient and robust tool in design of a partial admission turbine.

Introduction

The KARI (Korea Aerospace Research Institute) turbopump is under development as an essential component of KSLV (Korea Space Launch Vehicle) project. It consists of an oxidizer pump, a fuel pump with kerosene, a helium separator and a turbine system. Both pumps are coupled with a single shaft and driven by a turbine stage. Fig. 1 presents the three-dimensional view of the KARI turbopump.

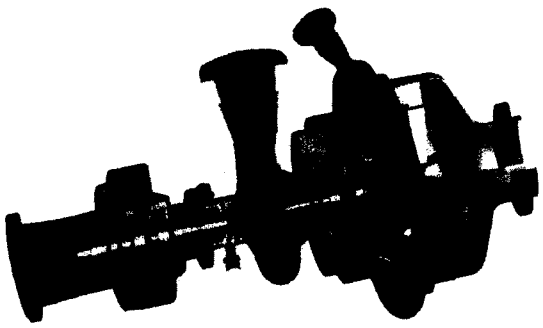

Fig. 1 Cutaway view of the KARI turbopump

The flow-field in a partial admission turbine is essentially unsteady due to the relative motion of rotor blade row and complex because of tip leakage and nozzle/rotor/stator interaction. It requires a three dimensional viscous and unsteady flow solver with tremendous data storage and time. Recently, some researchers[1] try to solve it directly. However, it is not popular in design phase.

One way to avoid, it is to resolve the steady flow-field on a computational domain formed by single blade passage. This requires a pitchwise averaging process at the pre-defined rotor/stator interfaces. This is so-called mixing plane approach. The rotor/stator interaction is done by exchanging the circumferential averaged flow quantities. As a result, physical properties are uniform in a pitchwise direction at the rotor/stator interface. It is true that a mixing plane technique has been widely used rotor/stator modeling in industry approach. However, it still remains the problem that how to define the representative values along the pitchwise direction physically. In a partial admission turbine case, the mixing plane method between nozzle and rotor is generally "not accepted" due to its strong pitchwise variation.

Unsteady rotor/stator interaction has been considered for a higher level of accuracy. Various techniques allowing to treat configurations with an arbitrary number of blades in the rotor and the stator have been proposed by many authors[2-4]. Each of them has its own characteristics, which affects the computing time and memory. Recently, the aerodynamic shape optimization, combined with an unsteady stator/rotor Navier-Stokes calculation is presented [5-6].

The domain scaling method is another type of unsteady rotor/stator interface treatment[7], based on the constraint that the pitch distance must be same on both boundaries of rotor and stator. If the numbers of blades of the rotor and stator are different, this implies either of two different numbers should be increased to scale the geometry. The method allows the arbitrary numbers of stator/rotor blades with an error proportional to the scaling factor. The accuracy of the computed unsteady flow solution may be improved by the expense of more data storage and CPU time when more blade passages are included.

The frozen rotor technique consists of a simple connecting boundary condition. The basic idea is identical to the domain scaling approach, except that the movement of rotor in the connecting algorithm is ignored. The governing equations are solved for the rotor in a rotating frame of reference, including

Coriolis and centrifugal forces in source terms, whereas the equations for the stator are solved in an absolute reference frame.

The two components are literally connected, and hence a rotor/stator approximation is not required. As a result, the final steady solution allows the pitchwise variation and the interface of stator/rotor is included in the computational domain. Due to this advantage, the frozen rotor method is said to be more accurate than the mixing plane. Though unsteady time effect such as the separated vortex shedding zone between nozzles can not be accounted, the frozen rotor method may be considered as an appropriate solution for analysis of a flow-field between nozzles and multiple rotor passages. In this present work, the frozen rotor method has been adopted to predict a performance of a partial admission turbine and survey pitchwise variations of the flow.

KARI Turbine Stage

The KARI turbine stage was designed to provide 1,620 kW at the rotational speed of 20,000 rpm. It composed of 14 converging-diverging nozzles, a single shrouded rotor disk with 103 impulse type blades and 33 EGVs (Exit Guide Vane). The pyro-gas is injected from two of 14 nozzles at the initial stage of turbine start to accelerate the rotational speed to the extent of 12,000 rpm. Then the turbine is driven with the rest of 12 partial admission nozzles injecting supersonic exhaust gas. Each injection nozzle except for the pyro-start has same pitch distance of 24 degrees. The nozzle geometry was determined by the characteristic equation not to produce strong gradient in the flow-field.

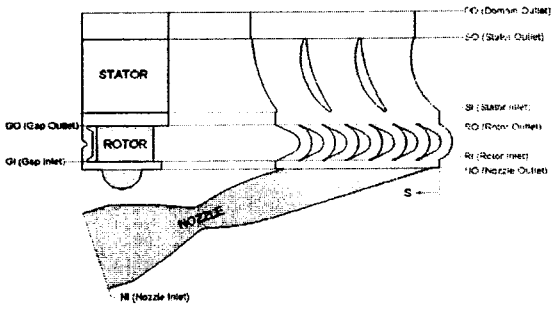

Fig. 2 Layout of the KARI turbine

The symmetric rotor shape was determined by four design parameters which are the lower and upper arc radii, leading edge thickness and blade angle[6]. The blade disk has 280 mm mean diameter and its velocity ration is 0.25. It is shrouded with a tip clearance of 2 mm. The tip clearance region of rotor is specially designed to reduce the tip leakage flow.

The profile of EGV can be generated by two arc radii and blade angle. The turbine is driven by a mixture of gaseous kerosene and oxygen with a ratio of specific heats, of 1.12 and gas constant, of 321. The gas enters the nozzles with a total temperature, of 900 K and a total pressure, of 5.78 MPa and a mass flow rate, of 4.9 kg/sec. Meanline calculations predict the Mach number at the exit of the nozzle to be about 2.4. The total to static pressure ratio across the nozzle was designed to be 14.45. The turbine layout and the position of reference planes are shown in Fig. 2.

Numerical Analysis

Computational Grid

To apply the frozen rotor method, the number of nozzles, rotor blades and EGVs were assumed to be 15, 105 and 45. The computational domain contained 1 nozzle, 7 rotor blade passages and 3 EGV passages with 1,988,595 node points. Each component has the same pitchwise periodic condition, and its phase angle is 24 degree. The rotor tip clearance is considered by adding a block. The entire grid is composed of H-type blocks. Table 1 summarizes the number of blocks and grid points used for each component. Fig. 3 represents meridian and 3-D view of the entire grid.

Table 1 Summary of grid dimensions

Component	Grid block	Grid points
Nozzle	6	164,606
Rotor	10	1,519,294
EGV	3	304,695
Total	19	1,988,595

(a) Three dimensional grid

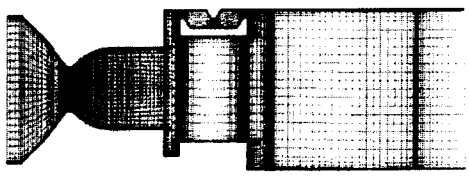

(b) Meridional view of the grid

Fig. 3 Computational mesh of the KARI turbine

Flow Solver

For numerical analysis, a commercial CFD software FINE^{TM}/Turbo was used. The EURANUS flow solver integrated in FINE^{TM}/Turbo solved the time dependent Reynolds Averaged Navier-Stokes equations on three dimensional multi-block structured grids. The space discretization was based upon a cell centered finite volume approach, used for central scheme. A density-based formulation was applied in flow regimes ranging from subsonic to hypersonic, whereas a preconditioning method was introduced to handle low speed and incompressible flows. The steady flow solution can be achieved by the convergence of four stage explicit Runge-Kutta integration scheme. To accelerate the residual convergence, a full mltigrid strategy, local time stepping and implicit residual smoothing are also implemented.

In the present work, turbulent flows were modeled with the Baldwin-Lomax algebraic model to reduce computing time. Because of the limitation of algebraic modeling, flow separation and vortex shedding may not be accurate. However it is still useful to survey the flow characteristics and performance. The full multigrid strategy of 3 levels was applied in order to create a good initial solution and it made solution converge faster.

Boundary Conditions

The total quantities of P_t = 5.78 MPa and T_t = 900 K were imposed at the nozzle inlet, NI (Nozzle Inlet) in Fig. 2 with the velocity direction of $V_x/|V|$ = 0, $V_r/|V|$ = cos 18° and $V_t/|V|$ = sin 18°. For the outlet conditions, a static pressure was prescribed at the domain outlet, DO in Fig. 2 with an averaged value of 0.4 MPa. Entire solid surfaces were treated as no-slip walls. The rotational speed of 20,000 rpm was given to the rotor solid surfaces. As a result, no-slip wall conditions in rotating coordinate corresponded to moving wall conditions in absolute reference coordinate. Due to the supersonic nozzle, the mass flow rate does not depend upon the prescribed static back pressure.

Results and Discussion

Predicted flow conditions at the inlet and the exit of the rotor and the entire computational domain are given in Table.2. Work per pound of gas is calculated using

$$\Delta h = Cp\, \Delta To \qquad (1)$$

Using the predicted flow conditions, the work per pound of flow is calculated to be 1980 kW, which is a bit high. Meanline analysis predicted 1670 kW. Power is defined as

$$PW = m\, \Delta h \qquad (2)$$

Predicted Mach number contours at mid-span are shown in Fig. 4. Subsonic flow enters the nozzle, chokes at the throat, and becomes supersonic. A Mach disk is seen downstream of the throat. Shock waves form in the diverging section and reflect off the nozzle walls. The fluid expands as it leaves the nozzle. Supersonic flow enters the blade, and a leading edge shock is formed.

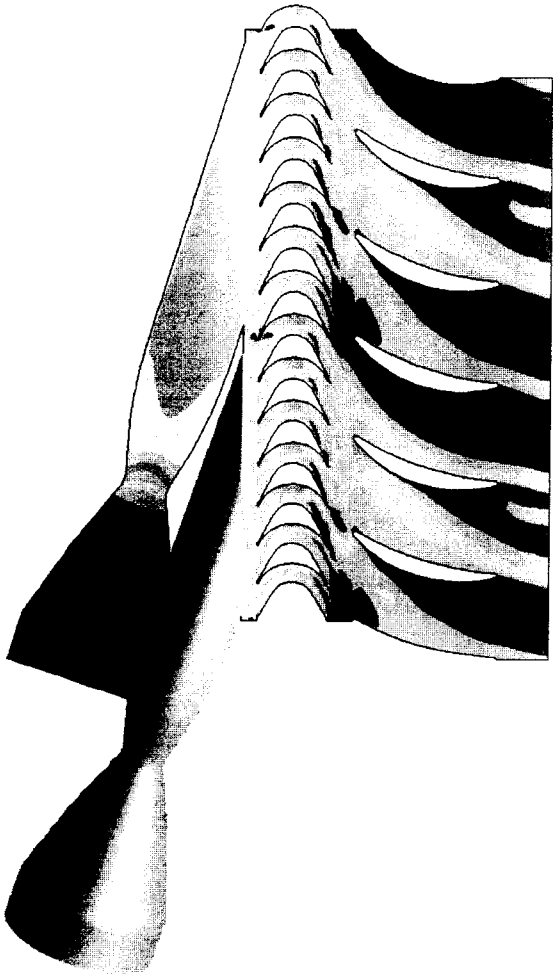

Fig. 4 Mach number contours at midspan

The boundary layer separates from the suction surface of the blade due to the interaction of the bow shock with the suction surface boundary layer. Mach number contours for rotor blade alone are shown in Fig. 5 to highlight the shock/boundary layer interaction. The separated region was expected as supersonic turbine blades generally generate large separated regions on the suction surface of the blade at design conditions. The size of the separation of the separation is dependent upon the blade's circumferential position relative to the nozzle. Because of the large separated region on the blade, the average Mach number at the exit of the blade is subsonic. The boundary layer on the suction surface of

EGV separates, and separation point is dependent upon the circumferential relative position to the nozzle.

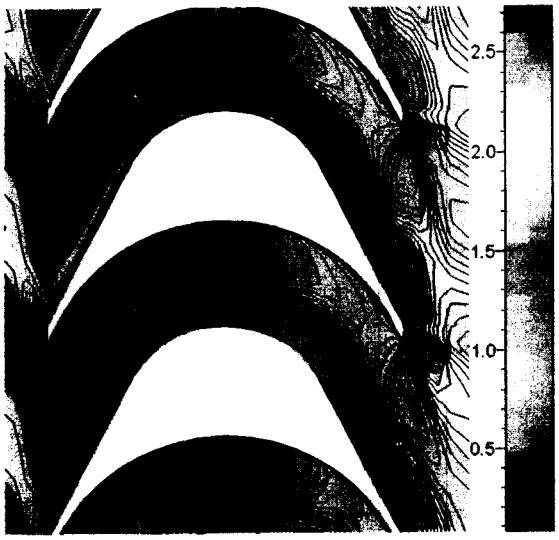

Fig. 5 Mach number contours at mid-span of rotor passages

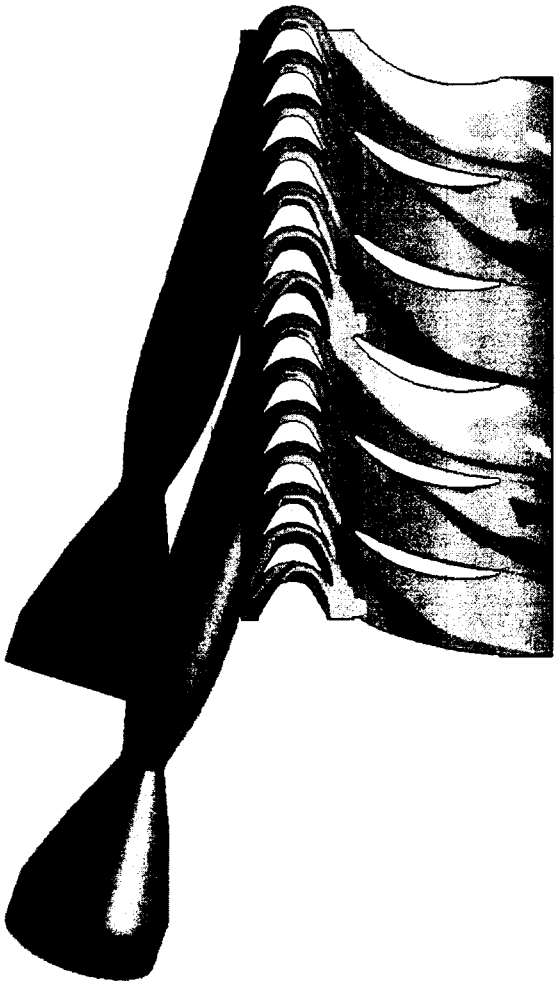

Fig. 6 Entropy contours near mid-span

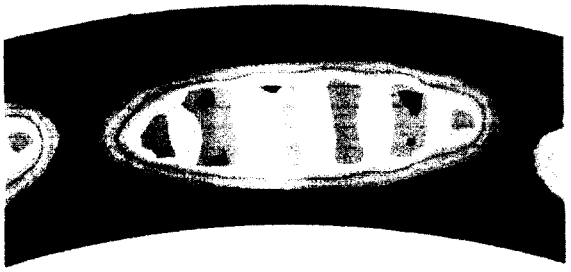

Fig. 7 Total pressure contours between nozzle exit and rotor leading edge

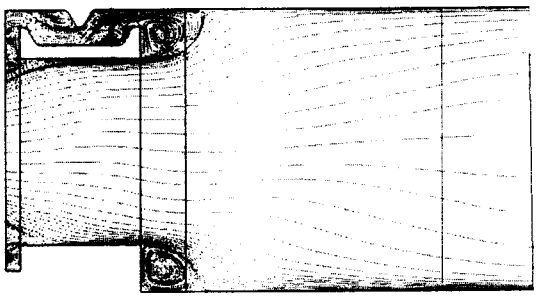

Fig. 8 Pitchwise-averaged velocity vector lines

To determine the mechanism of the increased separation on the blade and the separation on the suction side of EGV, instantaneous entropy contours are plotted (Fig. 6). The contours show a wake produced at the lip of each nozzle. This wake is due to the solid wall regions between each nozzle at the exit plane of the nozzle ring. This wake is chopped by an adjacent rotor blade, and it passed along the downstream direction. Finally, it strikes the stator and turns its direction toward the exit.

Fig. 7 shows an axial view of the total pressure contours between the nozzle exit and the blade leading edge to highlight the geometry and flow in this region. The nozzle lip wake triggers an earlier separation on the suction surface. The nozzle lip wake triggers an earlier separation on the suction side of the rotor blade than when the blade is fully within the nozzle jet (Fig. 6). When this boundary layer shed, this higher loss flow travels downstream, causing the separation on the suction side of the EGV. This physical phenomena has been known as a difficult issue in turbine designers because it is one of the major losses in calculating the turbine efficiency.

Fig. 8 represents the circumferential averaged streamlines on the meridian plane. As the flow leaves a nozzle, it expands along the spanwise direction slightly. Also, when it leaves the exit of the rotor blade, it expands again. In the axial gap region between the rotor and stator blades, two counter rotating vortices can be found at hub and tip. The vortex at tip causes an adverse flow direction in the tip clearance region, which is from trailing edge to leading edge of the rotor blade. Another reason comes from the prescribed static back pressure, which is higher than the static pressure at the nozzle exit. This

result is somewhat striking. It means that the amount of tip clearance does not affect the turbine efficiency much.

Fig. 9 illustrates the circumferential averaged physical properties along the streamline. Most of property changes occur in rotor blade. The supersonic flow at exit of the nozzle becomes subsonic after the rotor.

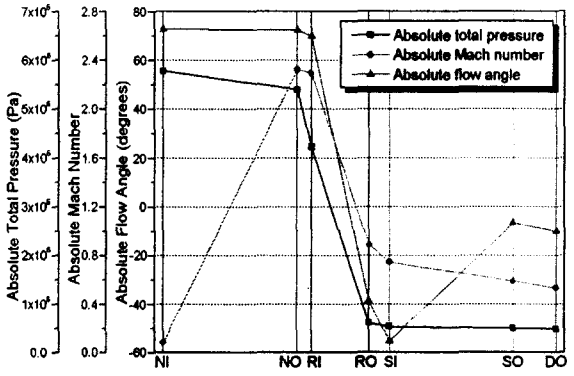

Fig. 9 Total pressure, Mach number, flow angle variations along the streamline

Table 2 Predicted results

Parameters		Nozzle		Rotor		Stator	
		NI	NO	RI	RO	SI	SO
Static pressure (Pa)		5757292	321812	256459	351649	349753	400598
Total pressure (Pa)	Absolute	5780000	5397726	3617719	536354	468378	443741
	Relative			1315708	912984		
Static temperature (K)		899.62	667.69	679.35	730.94	740.45	754.98
Total temperature (K)	Absolute	900.00	899.82	892.51	762.78	763.15	763.17
	Relative			804.13	803.84		
Mach number	Absolute	0.080	2.406	2.279	0.815	0.688	0.404
	Relative			1.730	1.260		
Flow angle (degrees)	Absolute	72.89	70.14	69.86	-38.39	-51.25	-6.51
	Relative			63.1	-62.11		

Table 2 summarized the predicted results. About 7 % of total pressure loss occurs at the nozzle due to the skin friction and Mach disk, and the rest of total pressure loss occurs at the rotor blade.

Fig. 10 represents the Mach number at rotor leading edge along the pitchwise direction. The coordinate *s* was defined in Fig. 2. The results of mixing plane show the same Mach number variation regardless of the position of the rotor blade. Discontinuities can be seen in each period because of the leading shock. The low Mach number region of frozen rotor corresponds to the lip of nozzle, and it results from the wake.

Mach number at hub is slightly higher than at tip. It results from the adverse flow at the tip leakage region. The mass flow through the tip leakage merged into the main nozzle flow, and it made the boundary layer at blade tip thicker. It can be clearly seen in Fig. 8. It is seen as if the nozzle flow leans toward the blade hub.

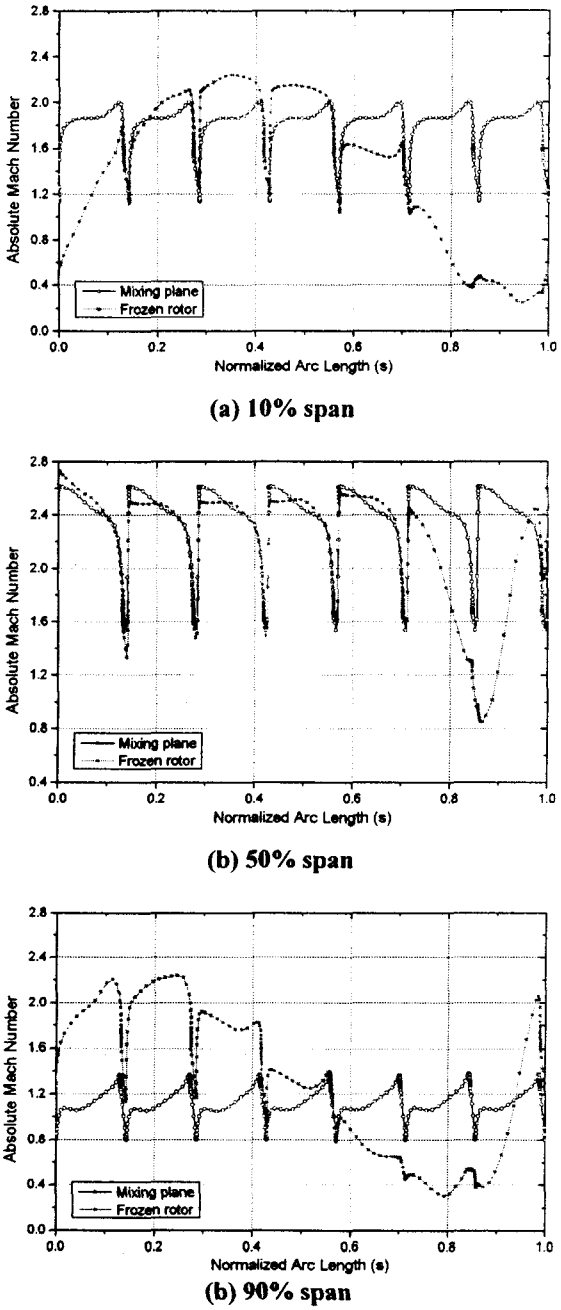

Fig. 10 Comparison of Mach number at rotor leading edge in pitchwise direction

Conclusion

A numerical study of the partial admission turbine was conducted. The results were used to support aerodynamic assessments and structural dynamics evaluations. By the use of the frozen rotor method, flow-field variation according to the circumferential position of rotor blades relative to the nozzle and stator were investigated.

The wake starting from the lip of the nozzle causes the large separation of the stator, and it is one of the

major characteristics of a partial admission turbine. The flow direction in tip leakage region turns out to be opposite to the main flow direction due to the isolated vortex behind the shroud and higher static pressure at the turbine exit than the nozzle exit. Also the mass flow coming from the tip clearance merged into the main nozzle flow, and it causes the flow direction through the rotor toward the downward. It is the opinion of authors that the tip clearance and pressure ratio of the turbine must be redesigned.

References

1) Griffin, L. W. and Dorney, D. J.: Simulation of the Unsteady Flow Through the Fastrac Supersonic Turbine, *Journal of Turbomachinery*, **122**, April 2000, pp. 225-233
2) Giles, M. B.: Stator/Rotor Interaction in a Transonic Turbine, *Journal of Propulsion*, 1990, pp. 621-627
3) Lemeur, A.: Calculus 3D stationnaire et instationnaire dans un étage de turbine transsonique, AGARD Report CP-510, 1992
4) Erdos, J. I., Alzner, E., McNally, W.: Numerical Solution of Periodic Transonic Flow Through a Fan Stage, *AIAA Journal*, **15** (11), 1977, pp. 1559-1568
5) Lee, E. S.: Rotor Cascade Shape Optimization with Unsteady Passing Wakes Using Implicit Dual Time Stepping Method, Ph. D. Thesis, Dept. of Aerospace Engineering, The Pennsylvania State University, August 2000
6) Lee, E. S. and Kim, J.: Numerical Studies of Geometrical Design Variables for Improvement of Aerodynamic Performance of Supersonic Impulse Turbine, The 12th International Conference on Fluid Flow Technology (CMFF'03), Budapest, September 2003, pp. 1246-1250
7) Rai, M. M.: Three-Dimensional Navier-Stokes Simulations of Turbine Rotor-Stator Interaction; Part I – Methodology and Part II – Results, *Journal of Propulsion*, **5** (3), 1989, pp. 305-319